

Original citation:

Mahmood, Arif, Small, Michael, Al-Maadeed, Somaya and Rajpoot, Nasir M. (Nasir Mahmood). (2017) Using geodesic space density gradients for network community detection. IEEE Transactions on Knowledge and Data Engineering, 294 (4). pp. 921-935.

Permanent WRAP URL:

<http://wrap.warwick.ac.uk/84012>

Copyright and reuse:

The Warwick Research Archive Portal (WRAP) makes this work by researchers of the University of Warwick available open access under the following conditions. Copyright © and all moral rights to the version of the paper presented here belong to the individual author(s) and/or other copyright owners. To the extent reasonable and practicable the material made available in WRAP has been checked for eligibility before being made available.

Copies of full items can be used for personal research or study, educational, or not-for profit purposes without prior permission or charge. Provided that the authors, title and full bibliographic details are credited, a hyperlink and/or URL is given for the original metadata page and the content is not changed in any way.

Publisher's statement:

"© 2017 IEEE. Personal use of this material is permitted. Permission from IEEE must be obtained for all other uses, in any current or future media, including reprinting /republishing this material for advertising or promotional purposes, creating new collective works, for resale or redistribution to servers or lists, or reuse of any copyrighted component of this work in other works."

A note on versions:

The version presented here may differ from the published version or, version of record, if you wish to cite this item you are advised to consult the publisher's version. Please see the 'permanent WRAP URL' above for details on accessing the published version and note that access may require a subscription.

For more information, please contact the WRAP Team at: wrap@warwick.ac.uk

Using Geodesic Space Density Gradients for Network Community Detection

Arif Mahmood, Michael Small, Somaya Ali Al-Maadeed, and Nasir Rajpoot

Abstract—Many real world complex systems naturally map to network data structures instead of geometric spaces because the only available information is the presence or absence of a link between two entities in the system. To enable data mining techniques to solve problems in the network domain, the nodes need to be mapped to a geometric space. We propose this mapping by representing each network node with its geodesic distances from all other nodes. The space spanned by the geodesic distance vectors is the geodesic space of that network. Position of different nodes in the geodesic space encode the network structure. In this space, considering a continuous density field induced by each node, density at a specific point is the summation of density fields induced by all nodes. We drift each node in the direction of positive density gradient using an iterative algorithm till each node reaches a local maximum. Due to the network structure captured by this space, the nodes that drift to the same region of space belong to the same communities in the original network. We use the direction of movement and final position of each node as important clues for community membership assignment. The proposed algorithm is compared with more than ten state of the art community detection techniques on two benchmark networks with known communities using Normalized Mutual Information criterion. The proposed algorithm outperformed these methods by a significant margin. Moreover, the proposed algorithm has also shown excellent performance on many real-world networks.

Index Terms—Complex Networks, Community Detection, Geodesic Space, Geodesic Distance, Density Field Gradients



1 INTRODUCTION

Many real world complex systems such as social networks on facebook and twitter, the internet and the web of hyper-links, connections between different components in an electric circuit and interactions of neural cells directly map to network data structures instead of geometric spaces. Therefore, network theoretic algorithms have often been used to analyze the structure of the underlying systems to study various network aspects such as interactions within the network, change propagation, edge and node density variations and resilience to targeted or random attacks. Often the edge and the node distribution is inhomogeneous in real-world networks resulting in node groups with high number of intra-group and low number of inter-group edges. These groups are referred to as communities and play an important role in the understanding of the structure of complex systems [37], [3].

Communities are the groups of entities in a network which share common attributes and often exhibit similar behavior. Community detection has the potential to solve many real world challenges such as identification of communities of clients having similar interests help in improving the service standards. The online community structure within social networks influences information propagation across the globe. The network of passengers traveling across countries define the spread of diseases across continents. A community of health workers and the patients

they handled share a level of exposure to the disease proportional to the intra-community links. Such communities are important for isolating possible carriers of contagious diseases such as the Ebola virus. Thus identification of network communities is an important topic across a number of research areas [14], [16].

Most existing community detection algorithms [8], [12], [18], [38], [42], [45], [46], [48] are graph theoretic and directly operate on the adjacency matrix. Most graph theoretic algorithms lack the ability to detect accurate community boundaries if the average difference between the internal and the external node degree does not exceed a strictly positive threshold [44]. Most of these methods use modularity [38], [17] as the quality index of a community. It has been observed that modularity maximization algorithms fail to identify communities smaller than a particular size even in cases when communities are well-defined [29]. The proposed community detection algorithm is fundamentally different from existing techniques as it is not based on modularity maximization. We experimentally observe that our proposed algorithm can detect communities at multiple resolutions. Also the detected community boundaries are more accurate even if the external node degree is the same as internal or even larger in some cases.

The proposed *Geodesic Density Gradient (GDG)* algorithm has three main steps. First we map a network to a geometric space, then we make the communities compact in that space by reducing intra-community distances and increasing inter-community gaps, and finally we cluster the nodes to get community labels. These steps have been shown as a block diagram in Figure 1. We map a network to a geometric space such that each node has a unique global position defined by a vector of geodesic distances from all other nodes. Geodesic distance is the shortest path distance between two nodes in the network. Geodesic distance vector contains shortest path distances between a node and all other nodes in the network. The choice of geodesic distance is motivated because of its ability to efficiently represent network

- A. Mahmood and S A Al-Maadeed are with the Department of Computer Science and Engineering, College of Engineering, Qatar University, Doha, Qatar. E-mails: {arif.mahmood, s_alali}@qu.edu.qa,
- M. Small is with the School of Mathematics and Statistics and the Complex Data Modelling Group, The University of Western Australia, WA 6009. Michael is also with Mineral Resources, CSIRO, Kensington, WA 6151. E-mail: michael.small@uwa.edu.au,
- Nasir Rajpoot is with the Department of Computer Science, University of Warwick, UK. E-mail: N.M.Rajpoot@warwick.ac.uk.

Manuscript received January 2016.

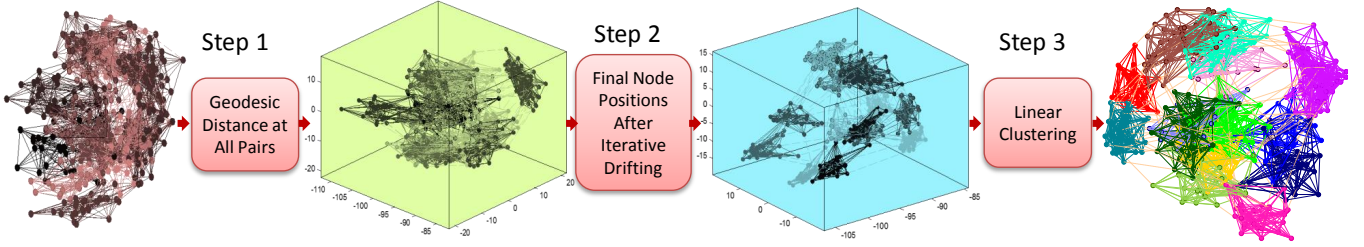


Fig. 1. Proposed algorithm has three main steps: for a given network geodesic distance at all pairs is computed and each node is represented by the corresponding vector of distances. In the geometric space, each node is drifted towards the local density maximum following a positive density gradient. A linear clustering algorithm is used to find an estimate of each maximum density region. All nodes drifting towards a particular region are assigned the same community label.

structure as recently shown by Mahmood and Small [35]. The space spanned by the geodesic distance vectors of a network is the geodesic space of that network. Distribution of nodes in the geodesic space encodes the network structure. Distance between two nodes in this space depends on the global position of these nodes in the network. The global network structure consists of global communities, while in many cases local network structure is also important to determine accurate local community boundaries. We propose a distance which incorporates both the global as well as local network structure for better discrimination between nodes belonging to the different communities especially on the community boundaries.

The motivation for the next step is to bring closer the nodes belonging to the same community, and move away the nodes belonging to the different communities. Purpose is compactness of communities and larger inter community gaps which will improve community detection performance. For this purpose, we consider each node in the geodesic space inducing a density field which is maximum at the node position and reduces as the distance increases. Density fields induced by all nodes get superimposed and therefore in certain regions of the space density becomes more compared to the other regions. This density distribution depends on the node distribution in the space which depends upon the network structure. Thus if the network structure varies, density distribution in geodesic space will also vary. For each node, we compute the direction of maximum positive density gradient and drift the node in that direction. Considering only one node at a time, the algorithm drifts all nodes one by one and then starts from the first node once again. The process is repeated until most of the nodes converge to regions with minimal density variation. These uniform density regions are also local maximum of the density field. It is because nodes have followed positive density gradients to reach these regions. The path followed by each node from its original position to the final position is a trajectory in the geodesic space (Figure 2). We observe that the nodes converging towards the same local maximum density region belongs to the same community in the original network. It is because of the network structure encoded in the geodesic space, the community structure translates into cluster structure. Our experiments show that the proposed algorithm can resolve communities at different resolutions much better than the traditional methods based on modularity optimization.

As a post processing step, clustering is required to be performed. It is because all nodes belonging to the same community do not converge to exactly the same position in the geodesic space. As a node drifts closer to a uniform density region, the density gradient gradually reduces to zero. Also the distribution of the density

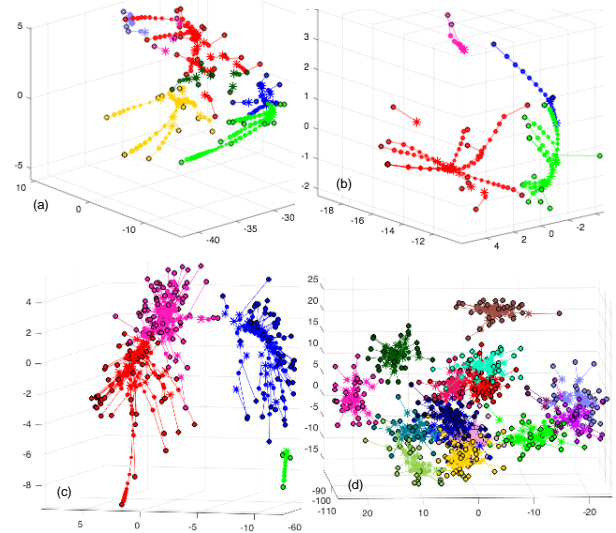


Fig. 2. In consecutive iterations of the step 2 of the proposed algorithm, nodes drift in the direction of positive density gradient and converge towards local density maximum regions. Initial position of a node is shown as circle and final position as ‘*’. Each community is shown in a different color. (a) Dolphins Network [33], [34] (b) Zachary Karate Club [50] (c) Jazz Bands Network [19] (d) LFR Benchmark [31] with 500 nodes and 13 communities.

gradient is not uniform around a maximum in the geodesic space causing nodes drifting from different directions to be stopped at different positions. By using a simple approach based on the k-means clustering algorithm we find clusters of nodes. A challenge with using the k-means algorithm is that it requires the number of clusters (unknown to us) as an input parameter. We solve this problem by varying the number of clusters and by observing the variation of clustering error derivative we can estimate an appropriate number of clusters in the network (see Figures 6 & 7). Note that other clustering algorithms such as DBSCAN [13] and OPTICS [2] do not require the number of clusters but do require other input parameters including the maximum distance (ϵ), and the minimum number of points ($MinPts$). There is no easy answer to fix appropriate values of these parameters.

To demonstrate the basic concept, an experiment was performed on an LFR network [31] with 500 nodes, 2500 links and 16 ground truth communities of size varying from 20 to 50 nodes (Figure 3). In the geodesic space nodes drift towards the positive density gradients. After convergence of nodes, final node positions are shown in Figure 4. One may observe that the compactness of communities has increased and inter community distances have

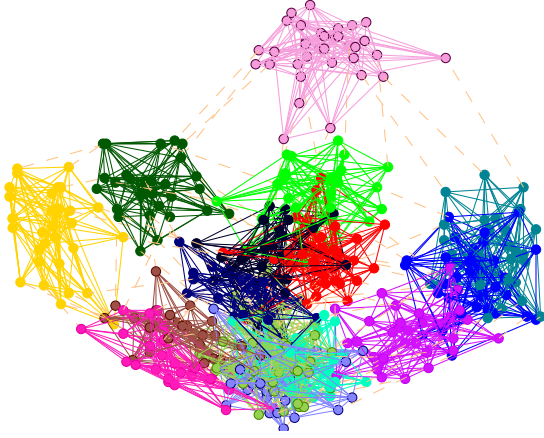


Fig. 3. An LFR benchmark network with 500 nodes, 2500 links used to demonstrate the proposed algorithm. Each node is represented by a 500 dimensional geodesic distance vector. For the purpose of visualization each node is projected on the three principal components using PCA. A 3D view of the network is rotated to clearly show all planted communities using different random colors.

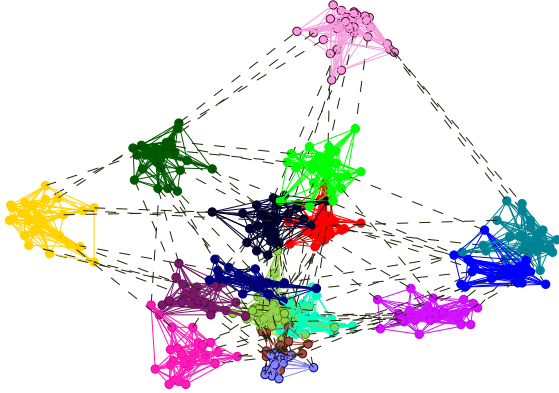


Fig. 4. The same network in Figure 3 after nodes have been iteratively drifted towards the local maximum density regions in the geodesic space. Communities have become more compact and inter-community distances have increased. Due to this step, significant performance gain is obtained compared to direct application of clustering techniques on the network shown in Figure 3. Using the proposed algorithm, we were able to find all 16 communities without any error.

increased making the community boundaries more distinct. This is one of the main reasons why we were able to obtain a better performance than the other algorithms which do not use this step. On the converged network, we applied k-means algorithm. As the number of clusters increased in the k-means algorithm, the clustering error decreased at a larger rate till $k = 16$. Beyond that the rate of decrease of clustering error was quite small. The 16 identified communities are shown in Figure 4 using different random colors. On the same network modularity maximization was also applied by varying the number of communities. Maximum modularity of 0.859 was obtained for 12 communities shown in Figure 5 using random colors. At least three communities contain visible sub-groups. This experiment shows that despite obvious structure, modularity maximization was not able to resolve all communities. In contrast, in this example, our proposed algorithm has accurately detected all communities without suffering from the resolution limit.

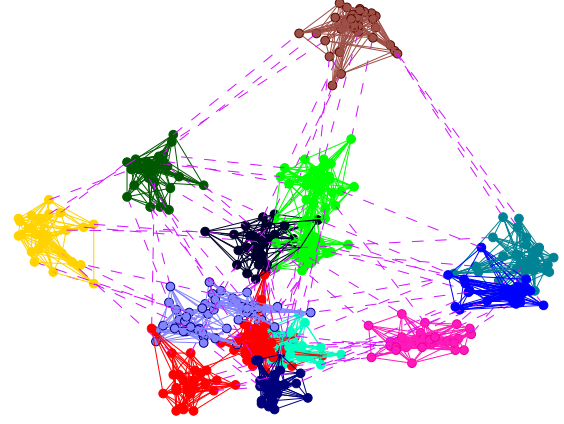


Fig. 5. For network of Figure 3 maximum modularity was obtained for 13 communities shown by different random colors. Each of the red, green and blue community has two groups of nodes. Despite an obvious community structure, modularity maximization failed to resolve all communities.

The idea of drifting nodes towards local density maxima in geodesic space is conceptually similar to the Mean Shift algorithm [7], [9]. However, to the best of our knowledge no similar algorithm has yet been applied to the problem of community detection in complex networks. In this direction, our contributions are several including a suitable distance for community detection in the geodesic space (Section 3.1), derivation of the estimate of the new node position using the proposed distance measure (Section 3.2), and estimation of the maximum density regions (Section 3.3). We also propose a technique to estimate suitable number of communities in a given network based on clustering error derivative (Section 3.4). Our experimental results will demonstrate the effectiveness of the proposed algorithm (Section 4). In the next section we give a brief overview of the related work.

2 RELATED WORK

We broadly arrange the important existing community detection methods in two groups. The methods in the first group use graph attributes to find communities. Methods in the second group map a network to a geometric space and then use pattern recognition techniques for community detection. Our proposed algorithm comes under the second group.

2.1 Graph Theoretic Algorithms

In this group of algorithms, network communities have been defined in a number of ways. S. V. Dongen considered a community to be a group of nodes if visited by a random walk, the walk will likely not leave the group until most of its vertices have been visited. He proposed Markov Cluster algorithm [48] based on the idea of current flow in the graph. If natural groups are present in the graph, then the current across group borders will be small thus revealing group structure in the graph.

Radicchi et al. [45] defined a strong community as a group of nodes with each node having more connections within the group than with the rest of the graph and a weak community has the sum of all degrees within the group larger than the sum of all degrees toward the rest of the network. They proposed a divisive algorithm based on edge-clustering coefficient, the ratio of number of triangles an edge belongs to the potential number of such

triangles. Edges connecting different groups have low clustering coefficient and are removed first.

Girvan and Newman [18], [38] proposed a community detection algorithm (GN) based on the concept of edge betweenness which is the number of shortest paths that run along an edge. The edge with highest betweenness is removed and shortest paths are recomputed each time. Clauset et al.[8] proposed a fast greedy modularity optimization algorithm which is very efficient on sparse graphs with hierarchical structure. Blondel et al.[4] proposed a modularity optimization based fast heuristic algorithms for community structure extraction in large networks.

Palla et al. [42] defined a community as a union of all k -cliques (complete subgraphs of size k) that can be reached from each other through a series of adjacent k -cliques (where adjacency means sharing $k - 1$ nodes). Their method first locates all cliques of the network and then finds the communities by carrying out a standard component analysis of the cliqueclique overlap. Chen and Saad [6] define communities as dense subgraphs.

Donetti and Munoz [12] have proposed DM algorithm which is spectral clustering for community detection. First a few eigenvectors of the network Laplacian matrix are computed and then based on Euclidean or angular distance existing algorithms are used to find clusters. Rosvall and Bergstrom has proposed an information-theoretic framework for resolving community structure in complex networks [47] known as Infomap. A network is divided into small modules such that Minimum Description Length (MDL) is minimized.

2.2 Mapping Networks to Geometric Spaces

Finding communities in complex networks by mapping to geometric spaces has not been well investigated. Nishikawa *et al* [41] used 28 node properties for feature space representation. Twenty of these properties are the eigenvector coefficients of the Laplacian and the normalized Laplacian matrices. Their method mainly leverages the strength of spectral clustering which maps data from nonlinear manifolds to linear space where data can be grouped by using k-means algorithm. Moreover, despite significant difference in the meaning of different features, the 28 dimensional feature vector is projected to random 2D space and the user is required to manually mark the clusters. The user input over different 2D views is combined to infer the community structure. In contrast to this approach, we represent a node with a feature vector containing the same type of distance from all other nodes in the network. Thus our approach is purely distance based and does not include node properties such a node degree or centrality which are not relevant to the notion of distance.

Jin *et al* [26] defined a distance function between two nodes based on the geometric mean of the costs of all paths between those nodes. Each node is assigned a density value as the sum of exponentially decaying influence functions. The node with maximum density value is selected to be the density-attractor and the nodes directly connected to it with lower density values are considered as the density-attracted. The embedding space is discrete considering only two nodes at a time. Another density based heuristic approach was proposed by Gong et al [20]. Similarity between two nodes was defined as the ratio of cardinality of the intersection to the union of the neighbors of the two nodes. All nodes in the neighborhood of a node with similarities larger than a threshold parameter are considered as one group. Recently Deritei *et al* [11] represented distance between two nodes based

on the edge-clustering coefficient and used Voroni diagrams for community detection. To the best of our knowledge, none of these algorithms have used the drifting of nodes towards positive density gradients to increase compactness of communities and improved discrimination by increased inter community distances as we propose before the clustering step. This is one of the main reasons our algorithm was able to achieve very good performance in almost all test cases.

In all of the existing approaches [11], [26], [20] network to geometric space mapping is considered for only two nodes at a time while the positions of the rest of the nodes in the geometric space are ignored. Since the assumed spaces are not continuous, therefore these are also not directly differentiable. None of these approaches are capable to represent complete network in the embedding space at the same time with an exception of Nishikawa *et al* [41]. They were able to represent network nodes in 2D space with the help of spectral clustering algorithm which acts as a non-linear to linear space transformation function. Therefore the projections shown by [41] are not the actual network representation rather a view after a transformation.

Recently Mahmood and Small [35] have proposed a subspace based network community detection algorithm. Their algorithm is based on the observation that each community only spans a subspace in the geodesic space. Sparse coding based approach was used to find community boundaries. The proposed concept works excellent for sparse networks. In real world dense networks due to the small world effect, the subspaces spanned by different communities become overlapped. To overcome this effect, information was leveraged from the traditional spectral clustering technique. Although the accuracy of their algorithm was better than the previous algorithms, the algorithm has high computational complexity.

Our proposed method is stochastic like the algorithm of Newman and Leicht (EM) [40] which is based on stochastic model to parametrize the probability of each possible configuration of group assignment. The likelihood of generating the observed network is maximized over the model parameters. However, in contrast to them we use k-means for finding cluster labels. Though k-means is a special case of EM on Mixture of Gaussians, our algorithm is much simpler than Newman and Leicht algorithm.

In contrast to the existing approaches, we propose to embed a network to a continuous geometric space using geodesic distance vectors. We consider path followed by nodes drifting towards the local density maximum to find the label of each node. To the best of our knowledge, no such network community detection algorithm has been proposed before. This work also bridges the gap between Data Mining and Complex Networks. Our algorithm is equally applicable to the weighted and directed networks, however we demonstrate results on unweighted and undirected networks which present a more difficult challenge.

3 PROPOSED ALGORITHM

The proposed *Geodesic Density Gradient (GDG)* algorithm has three main steps. First we map a network to a geometric space using geodesic distance vectors, then we make the communities in the geodesic space more compact by reducing intra-community distances and increasing inter-community gaps. Finally we cluster the nodes to get community labels. These steps has been shown as block diagram in Figure 1. In this section we will explain the

details of the theoretical challenges and our proposed solutions to handle these challenges.

Consider a graph G with n vertices and m edges represented by an adjacency matrix $A \in \mathbb{R}^{n \times n}$ such that if there is an edge between the two vertices $\{v_i, v_j\}$ then $A(i, j) = 1$, otherwise $A(i, j) = 0$ (assuming no self loops). The adjacency matrix as a whole captures the structure of the graph. The i -th column records the vertices directly incident on v_i and thus captures the local structure of the graph at the vertex v_i . Consider a mapping of vertices of G to a set of points P in an n dimensional geometric space such that each vertex v_i corresponds to a unique point $\mathbf{p}_i \in \mathbb{R}^n$.

We propose the vector \mathbf{p}_i to be the set of geodesic distances of v_i from each $v_j \in G$. Let $\mathbf{p}_i(j)$ be the shortest path distance between v_i and v_j . By the same notation, $\mathbf{p}_i(j) = 0$ if and only if $i = j$ (no self loops). In case of a fully connected graph each vertex v_i is reachable from any other vertex v_j , therefore the values in $\mathbf{p}_i(j)$ will be finite: $0 \leq \mathbf{p}_i(j) < \infty$. By using this mapping, no two distinct vertices in the same network can be mapped to exactly the same point in space. The space spanned by the geodesic vectors $\{\mathbf{p}_i\}_{i=1}^n \in \mathbb{R}^n$ is an n dimensional *Geodesic Space*, where n are number of nodes in the network.

3.1 Defining Distance in the Geodesic Space

Geodesic space is the space spanned by the geodesic vectors corresponding to the nodes of a particular network. In order to decide if vertices $v_i \in G$ and $v_j \in G$ belong to the same community, we consider two types of distances, a direct distance as the geodesic distance between v_i and v_j and an indirect distance induced by all other nodes in the network reachable from both of these nodes. Direct distance can also be considered as a local distance because it involves only two nodes. The indirect distance depends upon the global position of the two nodes with respect to all other nodes of the same network. Therefore, it may also be considered as a global distance. The direct distance is given by:

$$S_{i,j} = \frac{\mathbf{p}_i(j) + \mathbf{p}_j(i)}{2}. \quad (1)$$

In undirected networks $\mathbf{p}_i(j) = \mathbf{p}_j(i)$ and $S_{i,j} = \mathbf{p}_i(j) = \mathbf{p}_j(i)$. However, in case of directed networks geodesic distance may be different in both directions.

Considering the indirect distance $H_{i,j}$ between v_i and v_j , each vertex $v_k \in G$ where $k \neq \{i, j\}$ induces a component $\Delta H_{i,j,k} = \mathbf{p}_i(k) - \mathbf{p}_j(k)$. Overall indirect distance is given by

$$H_{i,j}^2 = \sum_{k=1}^{n-2} (\mathbf{p}_i(k) - \mathbf{p}_j(k))^2, \text{ s.t. } k \neq \{i, j\}. \quad (2)$$

Sum of both distances is given as $d_{i,j}$ where

$$d_{i,j} = \sqrt{\alpha S_{i,j}^2 + \beta H_{i,j}^2}, \quad (3)$$

where the parameters α and β scale the direct and the indirect distances. Note that for $\alpha = 2$ and $\beta = 1$, for undirected networks, the distance $d_{i,j}^2 = 2S_{i,j}^2 + H_{i,j}^2$ becomes Euclidean distance

$$d_{i,j} = \sqrt{(\mathbf{p}_i - \mathbf{p}_j)^\top (\mathbf{p}_i - \mathbf{p}_j)}. \quad (4)$$

However, in this case, the indirect distance becomes dominant over the direct distance and as a result global or coarse network structure gets more emphasis. On the other hand, selection of a large α and small β emphasizes local or fine structure of the network. We observe that an appropriate choice of these parameters

will emphasize an intermediate network structure which is more meaningful than the fine structure or the coarse structures. We can rewrite Equation (3) in vector form

$$d_{i,j} = \sqrt{(\Lambda(\mathbf{p}_i - \mathbf{p}_j))^\top (\Lambda(\mathbf{p}_i - \mathbf{p}_j))}, \quad (5)$$

where Λ is an $n \times n$ dimensional scaling matrix with $\Lambda_{ii} = \Lambda_{jj} = \sqrt{\alpha}$ and $\Lambda_{kk} = \sqrt{\beta}$ where $k \neq \{i, j\}$ as required by Equation (3). The distance between two nodes (5) in the geodesic space helps resolving community boundaries better than Euclidean distance or geodesic distance. Therefore, this distance (5) will be used for the derivation density field in the geodesic space.

3.2 Density Field in the Geodesic Space

Using geodesic distance vector, a network node v_j is mapped to a point \mathbf{p}_j in the geodesic space. A point \mathbf{p}_j may be considered inducing a continuous probability density field in the geodesic space. Assuming Gaussian probability density function with mean \mathbf{p}_j and isotropic variance b_w^2 , density at any point $\mathbf{p} \in \mathbb{R}^n$ due to a single node \mathbf{p}_j is given by

$$K(d_{p,j}, b_w) = \frac{1}{\xi} \exp \frac{-(\Lambda(\mathbf{p} - \mathbf{p}_j))^\top \Lambda(\mathbf{p} - \mathbf{p}_j)}{2b_w^2}, \quad (6)$$

where ξ is a normalizing factor ensuring unit summation over all \mathbf{p} . As \mathbf{p} moves away from \mathbf{p}_j , density will exponentially decrease with the increasing distance, where the definition of distance is as given by (5).

Density fields induced by all nodes of a network will get superimposed and generate a resultant density field in the geodesic space. Since the nodes belonging to the same community in the network form groups in the geodesic space, density will increase towards the center of the group. Therefore, group centers may be found by following the direction of positive density gradients. The community label of a node may be found by drifting that node in the direction of positive density gradient, until positive gradient vanishes in a region of local maximum density.

At any point $\mathbf{p} \in \mathbb{R}^n$ density induced by all nodes of a network is given by the summation of densities induced by individual nodes

$$\hat{f}(\mathbf{p}) = \frac{1}{nb_w^n} \sum_{j=1}^n K(\Lambda(\mathbf{p} - \mathbf{p}_j)/b_w), \quad (7)$$

where Λ is the scaling matrix defined in (5) for appropriately scaling of different dimensions in \mathbb{R}^n and $K(\cdot)$ is a non-negative scalar function with bounded energy. The parameter b_w is the bandwidth of the kernel function. Variation of the bandwidth parameter allows network analysis at different resolutions. If a differentiable kernel function similar to the one given by (6) is used, the gradient of the density estimate is given by

$$\nabla f(\mathbf{p}) = \frac{\Lambda}{nb_w^{n+1}} \sum_{j=1}^n \nabla K(\Lambda(\mathbf{p} - \mathbf{p}_j)/b_w), \quad (8)$$

where ∇ is a gradient operator with respect to each of the n spatial dimensions. Substituting the value of K from (6) in (8) and differentiating w. r. t. \mathbf{p} ,

$$\nabla f(\mathbf{p}) = \frac{\Lambda}{nb_w^{n+1}} \sum_{j=1}^n \frac{\Lambda(\mathbf{p} - \mathbf{p}_j)}{b_w^2} K(d_{p,j}, b_w). \quad (9)$$

The scaled and weighted average shift given by (9) is an estimate of the density gradient pointing in the direction of the maximum increase in the density. Iterating in the direction of the positive

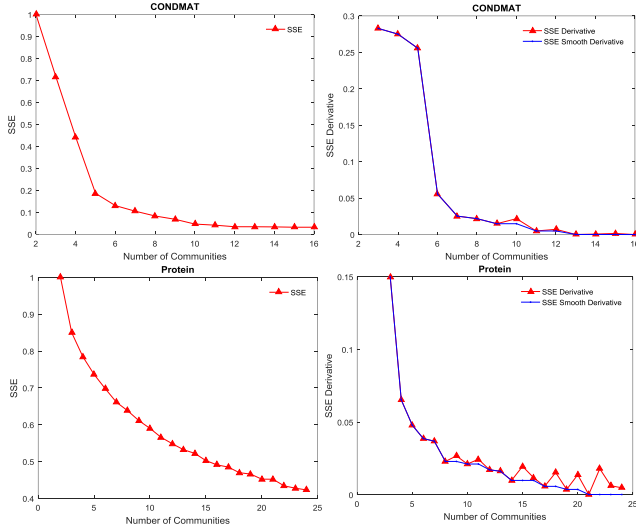


Fig. 6. Variation of SSE (14), derivative of SSE ($\delta\epsilon_k$) (15) and smooth derivative ($\widehat{\delta\epsilon}_k$) (16) with k for Cond Mat Col and Protein networks (see Table 1).

gradient, each node will converge towards a region of higher density. In this region the density gradient will approach zero because the density will be the same in all directions. Therefore, considering \mathbf{p} to be the current mode estimate, setting $\nabla f(\mathbf{p}) = 0$ we get the new estimate

$$\hat{\mathbf{p}} = \frac{\sum_{j=1}^n \mathbf{p}_j \exp\left(\frac{(\Lambda(\mathbf{p} - \mathbf{p}_j))^\top \Lambda(\mathbf{p} - \mathbf{p}_j)}{2b_w^2}\right)}{\sum_{j=1}^n \exp\left(\frac{(\Lambda(\mathbf{p} - \mathbf{p}_j))^\top \Lambda(\mathbf{p} - \mathbf{p}_j)}{2b_w^2}\right)}. \quad (10)$$

We repeatedly apply (10) to each node in the network resulting in a drift of each node in each iteration. As a result, nodes follow specific paths in the geodesic space. The final position of a node and its direction of movement are important clue for the community memberships. Iterations last until the ℓ_1 norm distance between the new and the old estimates $e_{t+1} = \sum_{j=1}^n \|\hat{\mathbf{p}}_j^{t+1} - \hat{\mathbf{p}}_j^t\|_1$ is less than a threshold showing that change in position of all nodes is insignificant.

3.3 Estimating Maximum Density Regions

As a node is drifted in the direction of positive density gradient, after a few iterations it will stop because density gradients will become very small in a region of local density maximum. We name the path followed by a node from its starting position to the stopping position as the *node trajectory* and the node stopping position as the *trajectory endpoint*. Most of the nodes do not converge to a single point rather stop at different positions in the maximum density region. In order to estimate boundaries of this region, we use a simple algorithm. We randomly pick a trajectory and find its nearest neighbor such that the distance between the two trajectories is minimum at the endpoints (node stopping positions). We simultaneously extend both trajectories as straight lines such that the perpendicular distance between them is minimized. The two nodes may not actually collide rather may pass close to each other. We compute the corresponding *nearest points* for all trajectory pairs and apply linear clustering on the *nearest points* and consider each cluster to span a region of maximum density. All

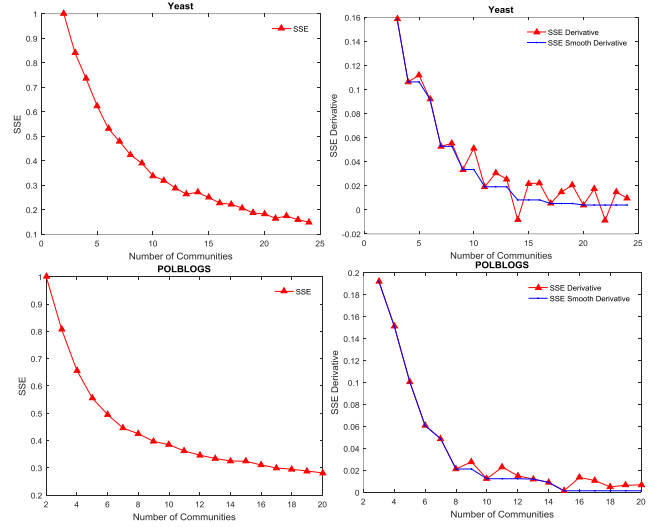


Fig. 7. Variation of SSE (14), derivative of SSE ($\delta\epsilon_k$) (15) and smooth derivative ($\widehat{\delta\epsilon}_k$) (16) with k for Yeast and Polblogs networks (see Table 1).

nodes converging towards a maximum density region are assigned the same community label.

Consider two trajectories with $\{\mathbf{p}_B, \mathbf{q}_B\} \in R^n$ as the trajectory endpoints. Let $\{\mathbf{p}_A, \mathbf{q}_A\} \in R^n$ be the points before the end points. Assuming in each of the following iteration, both nodes will keep on moving along the same straight lines with equal drift. In parametric form a point on each of these straight lines after t iterations is

$$\mathbf{p}_t = \mathbf{p}_B + t(\mathbf{p}_B - \mathbf{p}_A), \quad (11)$$

$$\mathbf{q}_t = \mathbf{q}_B + t(\mathbf{q}_B - \mathbf{q}_A). \quad (12)$$

Distance between the two lines after t iterations is $\mathbf{d}_t = \mathbf{p}_t - \mathbf{q}_t = \Delta_B - t(\Delta_B - \Delta_A)$ where $\Delta_A = \mathbf{p}_A - \mathbf{q}_A$, $\Delta_B = \mathbf{p}_B - \mathbf{q}_B$. Taking the derivative of squared distance function $\partial(\mathbf{d}_t^\top \mathbf{d}_t)/\partial t = 0$ we get the value of t_o for which error function is minimum:

$$t_o = \frac{\Delta_B^\top (\Delta_B - \Delta_A)}{\|\Delta_B - \Delta_A\|_2^2}. \quad (13)$$

Substituting value of t_o in (11) and (12) the values of nearest points $\{\mathbf{p}_o, \mathbf{q}_o\}$ is computed. If the two trajectory end points are very close to each other, then $\Delta_B \approx 0$ resulting in $t_o = 0$ meaning the trajectory end points are the nearest points.

3.4 Estimating the Number of Communities

K-means clustering is used as a post processing step to divide the nearest points (defined in the Subsection 3.3) to k clusters. In many real world networks the division of nearest points into well-defined groups is challenging, especially when k is unknown. Note that other clustering algorithms such as DBSCAN [13] and OPTICS [2] can also be used at this step. However none of the clustering algorithm is parameter free. K-means requires the number of clusters to be input by the user, DBSCAN and OPTICS both need maximum distance (ϵ) and minimum number of points (*MinPts*) to be provided by the user. Also the shape of maximum density regions resulting by summation of Gaussians is linear and therefore a non-linear clustering algorithm may not result in significant performance boost.

K-means objective function is Sum of Squared Error (SSE). SSE for k clusters given by

$$\epsilon_k = \sum_{j=1}^k \sum_i (\mathbf{p}_{ji} - \mathbf{c}_j)^\top (\mathbf{p}_{ji} - \mathbf{c}_j), \quad (14)$$

where \mathbf{p}_{ji} is a data point having nearest cluster center \mathbf{c}_j , therefore considered member of j -th cluster. In general, as k is increased, ϵ_k will decrease and eventually becomes zero when the number of clusters equals the number of data points. Figures 6 & 7 show the variation of SSE with k for four networks. In these networks, there is no clear indication on the plots when the clustering must be stopped.

Discrete derivative of the objective function (14) w.r.t. k is given by

$$\delta\epsilon_k = \frac{\epsilon_k - \epsilon_{k+\delta k}}{\delta k}, \quad (15)$$

where $\delta\epsilon_k$ is SSE derivative. We empirically observed that SSE derivative rapidly decreases from $k = 2$ to a larger value, then it becomes a bit transient as k approaches the actual number of clusters in the network. This behavior of SSE derivative is shown in Figures 6 & 7 for four networks.

We propose a simple smoothing function for the SSE derivative such that it becomes monotonic decreasing function of k . If the current value of $\delta\epsilon_k > 0$ is larger than a previously seen value of $\delta\epsilon_{k-p} > 0$, where $p > 0$ is a positive number, then replace the current value with the previously seen minimum value.

$$\widehat{\delta\epsilon}_{k+1} = \begin{cases} |\delta\epsilon_{k+1}| & \text{If } |\delta\epsilon_{k+1}| \leq \widehat{\delta\epsilon}_k \\ \widehat{\delta\epsilon}_k & \text{Otherwise} \end{cases}, \quad (16)$$

where $\widehat{\delta\epsilon}_{k+1}$ is smooth SSE derivative. The required number of clusters k^* corresponds to k beyond which $\widehat{\delta\epsilon}_k \leq \epsilon_{th}$, where ϵ_{th} is a small positive threshold. In networks with not a good clustering structure, $\widehat{\delta\epsilon}_k$ may not approach the ϵ_{th} . In those cases if $\widehat{\delta\epsilon}_k$ remains unchanged for a particular number of clusters. We assume that the appropriate number of clusters has already been achieved when the minimum value of $\widehat{\delta\epsilon}_{k+1}$ was obtained.

In Figure 6, for the case of the Protein network, reduction of SSE smooth derivative beyond 21 communities is negligibly small $\widehat{\delta\epsilon}_{21} \leq \widehat{\delta\epsilon}_3/100$, therefore algorithm selected $k^* = 21$. In Figure 7, for the case of Yeast network, $\widehat{\delta\epsilon}_{20} \leq \widehat{\delta\epsilon}_3/40$ however for $k > 20$, smooth derivative remains the same for the next four values of $k = \{21, 22, 23, 24\}$. Therefore, algorithm selected $k^* = 20$ for the Yeast network.

3.5 Complexity Analysis of the Proposed Algorithm

The proposed algorithm has three main steps: computation of geodesic distances, drifting each node towards a local density maximum, and finally the use of k-means community label assignment. Complexity of each step has been analyzed separately.

The presence of very fast algorithms for computation of shortest paths between all pairs of nodes in a network motivates our choice of using geodesic distances for mapping a network to a geometric space. Pettie and Ramachandran [43] have proposed an algorithm for the all-pairs geodesic distance problem having the time complexity of $O(mn \log \alpha(m, n))$, where $\alpha(m, n)$ is a very slowly growing inverse-Ackermann function, m is the number of edges, and n is the number of vertices. Recently Jiang et al. [25] has proposed Quantum Bosonic Shortest Path Searching (QBSPS). For the all-pairs shortest-path problem in

a random scale-free network with n vertices, QBSPS runs in $O(\mu(n) \ln \ln n)$ time [25].

A simple implementation of the algorithm used in step 2 of the proposed approach has time complexity of $O(dtn^2)$ where d is the dimensionality of the space, t is the number of iterations and n is the nodes in the network. We observe that algorithm converges quickly, mostly in less than five iterations $t \leq 5$. More efficient implementations of this step are possible by using bucket data structure [27].

Number of iterations may be reduced by using a simple heuristic that if a node comes within a small distance of another node then both will end up in the same final position. Therefore, a previously computed result may be reused. Complexity may further be reduced by using the locality constraint. If a node n_i has a final position $\hat{\mathbf{p}}_i$, then all nodes which are initially within a small distance of n_i will also end up very close to $\hat{\mathbf{p}}_i$. Therefore, these nodes may be assigned the same community label as n_i .

For scalability of the algorithm to larger networks, the dimensionality of the space has to be reduced by using appropriate dimensionality reduction techniques. We performed some experiments using PCA as the dimensionality reduction technique (see Section 4.6). In addition to all these speedup techniques, a parallel implementation of the algorithm can also significantly reduce the execution time.

Computing PCA is equivalent to computing SVD of a matrix. Exact SVD of an $m \times n$ matrix has time complexity $O(\min\{mn^2, m^2n\})$. In case of geodesic distance matrix of size $n \times n$, time complexity of SVD is $O(n^3)$. It is one-time cost in the proposed algorithm and may be performed offline. Therefore, it is feasible for networks with couple of thousands of nodes. For larger networks with millions of nodes, randomized algorithms may be used. Halko et al. [24] have used a randomized version of the block Lanczos method for computing SVD of large matrices having time complexity $O(ikN_a + i^2k^2n)$, where $i \leq 2$, k is the number of principal components to be computed, N_a is the number of non-zero entries in the matrix.

The third step of the algorithm is post processing of the results generated by step 2. We apply k-means repeatedly with increasing number of clusters until cluster error rate becomes less than a threshold. If there are k communities in the network, then k-means will be applied less than k times. Starting with a better initial estimate will reduce the number of iterations. The running time of Lloyds k-means algorithm, that we used in this work has time complexity of $O(nkdt)$, where n is the number of nodes, k the number of clusters, t the number of iterations needed until convergence, and d is the dimensionality of the space.

Thus the dominating factor of time complexity of the proposed algorithm is $O(dtn^2)$ in step 2 of the algorithm. The space complexity of the proposed algorithm is $O(dn)$ because we have to store n vectors each of dimensionality d .

4 EXPERIMENTS AND RESULTS

Proposed algorithm is named as *Geodesic Density Gradient (GDG)* algorithm for community detection. For all experiments the values of $\alpha = 1/2$ and $\beta = 1/(n-2)$ are used in (3) where n is the number of nodes in the network. This is because the indirect distance has $(n-2)$ dimensions and the direct distance has only two dimensions. These values of α and β ensure both distances become normalized over the number of dimensions. The value of the band-width parameter b_w in (10) also produces a scaling

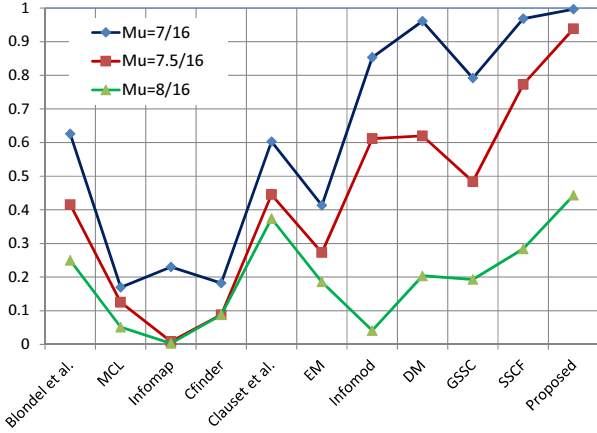


Fig. 8. Normalized Mutual Information (NMI) obtained by different algorithms averaged over 100 realizations of GN benchmark network for each value of Mixing Parameter $\mu = \{7/16, 7.5/16, 8/16\}$, where 16 is the total degree of each node. The proposed Geodesic Density Gradient (GDG) algorithm has obtained cumulative 35.36% more accuracy than SSCF which is the existing best performing algorithm.

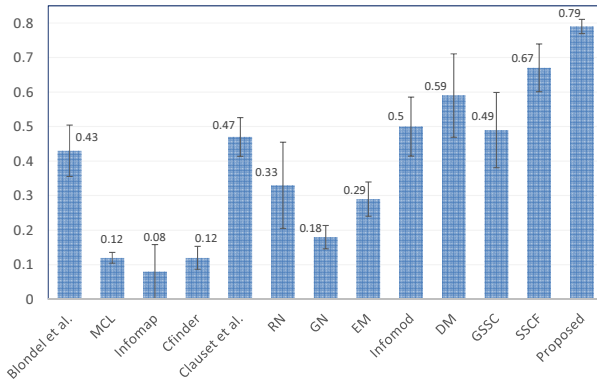


Fig. 9. Overall Average Normalized Mutual Information (NMI) obtained by different algorithms over 300 realizations of GN benchmark network. The proposed SGA algorithm has obtained on the average 11.78% more accuracy than SSCF, the existing best performing algorithm.

effect. For the above mentioned values of $\alpha = 1/2$, $\beta = 1/(n-2)$, $b_w = 1$ yielded the best performance.

The GDG algorithm is compared with the existing state of the art methods on two standard benchmark networks with known communities. The performance is compared with 12 existing algorithms including fast modularity optimization by Blondel et al. [4], Markov Cluster algorithm (MCL) [48], Infomap [47], Cfinder [42], fast greedy modularity optimization by Clauset et al. [8], Radicchi et al. [45], algorithm of Girvan and Newman (GN) [18], [38], spectral algorithm by Donetti and Munoz (DM) [12], Expectation-Maximization (EM) algorithm by Newman and Leicht (EM) [40] and Potts model approach by Ronhovde and Nussinov (RN) [46]. In addition to these algorithms comparisons are also performed with two recent algorithms including Geodesic Sparse Subspace Communities (GSSC) and Sparse Subspace Communities with Fusion (SSCF) [35]. Experiments are also performed on ten real-world networks.

4.1 Comparisons on GN Benchmark Network

The Girvan-Newman (GN) benchmark [18] has regularly been used to compare the performance of different community detection

algorithms [10], [28]. The network has 128 nodes and four planted ground truth (GT) communities of equal size. Each node has probability p_{in} of being connected to the nodes of the same community and p_{out} of being connected to the nodes of the outside communities. Since the degree of a node is fixed to 16, therefore only one of these two parameters is independent. A mixing parameter μ is defined as the ratio of the external degree of a node to the total degree. For example, $\mu = 7/16$ means for each node out of 16 links, 7 links are to the outside world. For small values of μ the structure is well-defined, while for $\mu \geq 0.50$, $p_{out} \geq p_{in}$, the graph becomes random with subtle structure.

Experiments are performed by varying the mixing parameter $\mu = \{7/16, 7.5/16, 8/16\}$. In each setting, 100 realizations of the benchmark are used to find an average Normalized Mutual Information (NMI) [10], [30] between the ground truth and the obtained communities. The proposed algorithm has obtained an $NMI = \{0.997 \pm 0.0721, 0.938 \pm 0.0758, 0.443 \pm 0.0820\}$ respectively.

The NMI comparison is shown in Figures 8 & 9. For all values of $\mu < 7/16$ the proposed GDG algorithm was obtained $NMI \approx 1.00$, showing 100% accuracy. For $\mu = 7/16$ we obtained average NMI of 99.66% which is higher than all other algorithms under consideration. For $\mu = 8/16$, performance of most algorithms significantly decreased however the proposed GDG algorithm was able to achieve average NMI of 93.83% which is again significantly larger than all other algorithms.

On this benchmark, on the average, SSCF algorithm of Mahmood and Small has remained the second best and the spectral clustering algorithm of Donetti and Munoz (DM) [12] is the third best algorithm. DM was able to obtain good accuracy by using angular distance and complete linkage clustering (see Figure 3 in [12]). Also the number of nodes in this network are only 128 and degree of each node is very high. Due to the small world effect, maximum geodesic distance in typical GN networks is ≤ 3 . Despite these challenges, the GDG algorithm has performed better than the rest of the existing algorithms including subspace based community detection with fusion (SSCF).

We use T-test to evaluate the statistical significance of the hypothesis that the proposed GDG algorithm is on the average more accurate than the closest competitor SSCF algorithm on GN benchmark. Because the sample is 100 random networks in each of the three settings, degree of freedom is 99 and the computed value of t is $\{3.564, 9.473, 9.360\}$ respectively for $\mu = \{0.60, 0.65, 0.70\}$. Using our results, the hypothesis is statistically significant for $p\text{-value} \leq 0.05\%$ for all settings.

4.2 Comparisons on the LFR Benchmark

The Lancichinetti-Fortunato-Radicchi (LFR) benchmark [31] has power law degree distribution and community sizes are also variable, presenting more challenges to the community detection algorithms. In this experiment, the number of nodes in the network is 1000, the average degree is 20 and the maximum degree is 50. Minimum ground truth community size is 30 and maximum is 100. Therefore, the number of ground truth communities may vary from 10 to 33. The mixing parameter is varied $\mu = \{0.60, 0.65, 0.70\}$. For each setting, 100 networks are randomly generated by using the implementation of the original authors [28]. The detected communities are compared with the ground truth by using NMI [30]. The proposed algorithm has achieved $NMI = \{0.834 \pm 0.0710, 0.600 \pm 0.0759, 0.240 \pm 0.0662\}$ respectively for the three mixing parameter values. For the EM

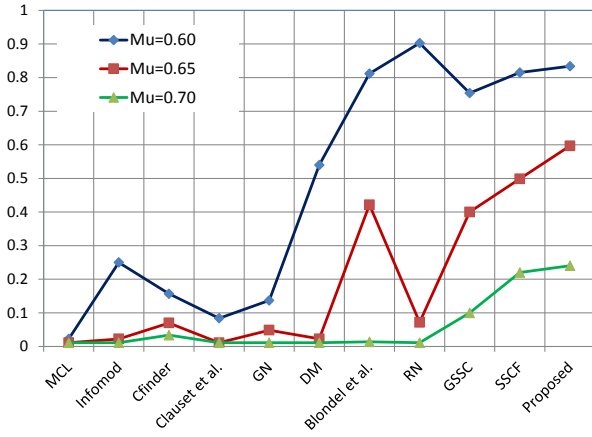


Fig. 10. Normalized Mutual Information (NMI) obtained by different algorithms averaged over 100 realizations of LFR benchmark network for each value of the Mixing Parameter $\mu = \{0.60, 0.65, 0.70\}$. Overall accuracy improvement of the proposed GDG algorithm is 13.73% over the existing best performing algorithm SSCF of Mahmood and Small.

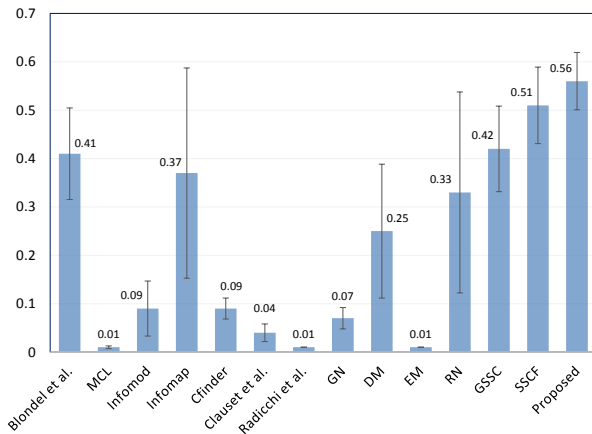


Fig. 11. Average Normalized Mutual Information (NMI) obtained by different algorithms over 300 realizations of LFR benchmark network. Average accuracy improvement of the proposed GDG algorithm is 8.10% over the existing best performing algorithm SSCF of Mahmood and Small.

algorithm, results are reported for the random initialization. Due to variable degree, communities of different sizes and increased mixing parameter, the performance of all algorithms has reduced compared to GN benchmark. An NMI comparison for different algorithms is shown in Figures 10 and 11.

The performance of subspace based community detection GSSC algorithm has improved on this benchmark and it has become the second best algorithm. It is because of increased number of nodes and comparatively lower average node degree. The performance of DM [12] algorithm has significantly deteriorated due to more challenges. Other algorithms including Blondal et al., infomap and RN performed better for $\mu = 0.60$ while for $\mu = 0.65$ only the algorithm of Blondal et al. has shown comparatively good performance. For $\mu = 0.70$ all existing algorithms except GSSC and SSCF have shown almost zero performance. It is because the modularity based methods perform poor when the community size reduces and the network size increases [15]. Also for zero or negative detectability thresholds, the performance of these methods deteriorate. The proposed GDG algorithm has

TABLE 1

Results of the proposed GDG algorithm on 11 real-world networks, n, m are the number of nodes and edges, M, k_m are the maximum modularity and corresponding number of communities, $\epsilon_k/\epsilon_2, k$ are the normalized clustering error and corresponding communities.

Network	n, m	M, k_m	$\epsilon_k/\epsilon_2, k$
Dolphin [33], [34]	62, 159	0.5, 6	0.08, 16
Jazz [19]	198, 2742	0.43, 4	0.12, 14
Coauthorships [39]	379, 914	0.79, 13	0.13, 13
Technology [5], [36]	512, 819	0.70, 6	0.25, 19
Asia MidEast [21], [22]	706, 2572	0.56, 7	0.23, 13
POLBLOGS [1]	1490, 9545	0.78, 3	0.32, 15
Protein [23]	1458, 1970	0.71, 20	0.45, 21
Yeast [36]	622, 1062	0.70, 13	0.16, 20
Global Air [21], [22]	3618, 14142	0.55, 11	0.33, 13
WestPower Grid [49]	4941, 6594	0.83, 13	0.00, 24
Cond Mat Col [32]	23133, 93497	0.75, 2	0.03, 13

obtained 24.03% NMI for $\mu = 0.70$ which is an improvement over the current best method. More accuracy of GDG algorithm for $\mu = \{0.65, 0.70\}$ shows the capability of the approach to accurately detect communities in more challenging situations.

We use T-test to evaluate the statistical significance of the hypothesis that the proposed GDG algorithm is on the average more accurate than the closest competitor SSCF on LFR benchmark. Because the sample is again 100 networks therefore DOF is 99 and we found $t = \{2.256, 8.721, 2.89\}$ respectively for the three settings. Using our results, the hypothesis is statistically significant for p-value $\leq \{2.5\%, 0.05\%, 0.5\%\}$ respectively.

4.3 Experiments on Real-World Networks

In real-world networks, there is no ground truth node labeling therefore it becomes difficult to compare the accuracy of the proposed algorithms with the existing methods. Also most of the existing methods try to maximize modularity which has recently been found to not be capable of resolving communities of smaller sizes. Therefore we report both the modularity M and the clustering error ϵ_k corresponding to minimum error derivative (Table 1). For each network, we normalize the k-means clustering error over two clusters (ϵ_2) to 1.00 and scale the error over $k > 2$ clusters as ϵ_k/ϵ_2 . Results are reported for GDG algorithm with fixed value of $b_w = 1/\sqrt{2}$.

Experiments are performed on eleven real world networks and the results are summarized in Table 1. Number of nodes in these networks vary from 62 to 23133. For each network we compare the communities found by maximum modularity with those found by the proposed algorithm. The structure of the five of these networks is shown in the geodesic space along with communities in Figure 12.

In the networks with well-defined community structure, the ϵ_k/ϵ_2 is significantly smaller than 1.00. For example consider Western United States Power Grid Network [49] having 4941 nodes and 6594 edges (Table 1). This network represents the topology of the power grid. An edge is a power supply line and a node is either a generator, a transformer or a substation. Figure 13b shows the initial node positions when the network was mapped to the geodesic space. Figure 13a shows the final node positions after each node has been converged to the region of maximum density. Nodes belonging to the same communities have converged to very small regions in the geodesic space. Very compact communities

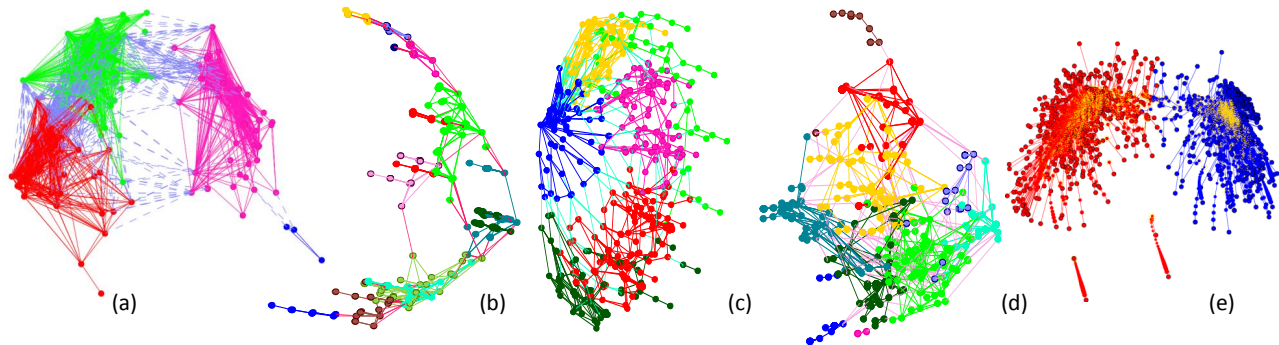


Fig. 12. (a) A two level hierarchical structure of the Jazz Bands network. The two main partitions correspond to bands in the New York and Chicago and further division shows the segmentation of black and white bands in each partition. (b) Largest connected component of Coauthorship network consisting of 13 communities. (c) Electronic circuits network. (d) Transcription Yeast network. (e) POLBLOGS network showing two main groups in 2004 US election. Tracks of node movements are also shown.

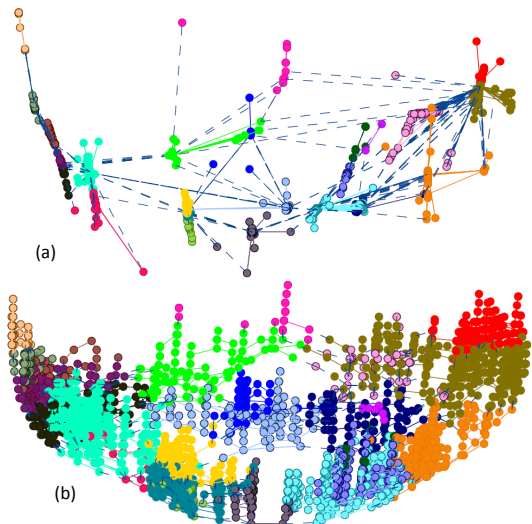


Fig. 13. Western Power Network has exhibited very strong community structure with almost zero residual error for 24 clusters (b). Trajectory end points after convergence.

can be viewed in Figure 13a. For this network, for 24 communities shown by different colors in Figures 13a and 13b, $\epsilon_{24}/\epsilon_2 < .005$.

The Condensed Matter network (COND-MAT) [32] with 23,133 nodes and 93,497 edges also has a well-defined community structure (see Table 1). This network covers scientific collaborations between authors of papers submitted to the Condensed Matter category in arXiv. The nodes indicate authors and the links indicate co-authorship's. For this network in our algorithm $\epsilon_{13}/\epsilon_2 < 0.03$ indicates that network has 13 compact communities. Maximum modularity of 0.75 was obtained for only two communities. Thus for this network, modularity maximization has completely failed to capture the network structure because network definitely have large number of communities.

The Technology Graphs [5], [36] are constructed from electrical circuits, where nodes represent logic gates and flip-flops. The 6 communities shown in Figure 12c correspond to maximum modularity of 0.70. In the geodesic space, this network has a conical structure which is open from one side. All nodes close to the apex of the cone are in one community, the surface of the cone is divided into five communities and protruding nodes have formed the 6-th community. The number of communities corresponding to minimum smooth error given by (16) is 19 and the corresponding $\epsilon_{19}/\epsilon_2 < 0.25$, which shows that this network

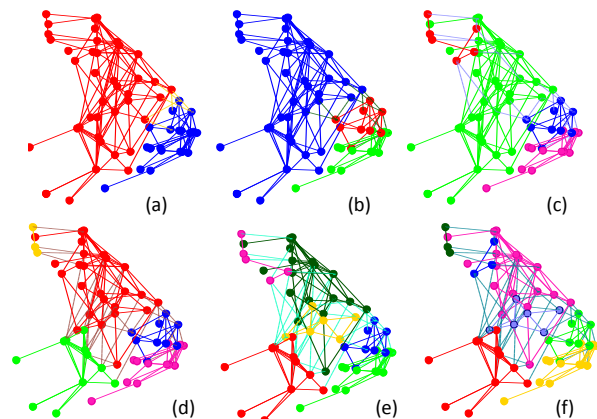


Fig. 14. GDG Algorithm: (a-f) hierarchical structure of the Dolphins network is revealed by increasing clusters from two to seven. Each time clustering is independently performed but the cluster boundaries are mostly preserved, demonstrating stability of the communities.

has a weak community structure.

4.4 Hierarchical Structure

The proposed GDG algorithm can also reveal hierarchical structure of a network, if such structure exists. For example, hierarchical structure of the Dolphin social network [33], [34] is revealed when the number of communities is increased from 2 to 7 (Figure 14). Similarly, two level hierarchical structure of Jazz Bands Network [19] is shown in Figure 12a.

Zachary Karate Club [50] is one of the commonly used network for community detection experiments. This network represents friendships between the 34 members of a karate club and has 77 links. By increasing the number of communities (K) from 2 to 6 we observe a hierarchical structure in this network (Figure 15). For $K = 2$ the two detected communities are marked as L and R in Figure 15. These communities are exactly the same as the club later broke down. We observe split of a small community $\{3, 9, 14, 21\}$ in Figure 15 such that $\{3, 14, 20\}$ are part of the administrator group (with node 1) and $\{9\}$ is the part of the instructor group (with node 33). As the number of communities is increased to 3, L split into $L1$ and $L2$ while R remained intact. However with $K = 4$, R also split into $R1$ and $R2$ communities. This reveals a perfect hierarchical structure in this network. For $K = 5$, we observe a split of $L1$ into $L1a$ and $L1b$ communities.

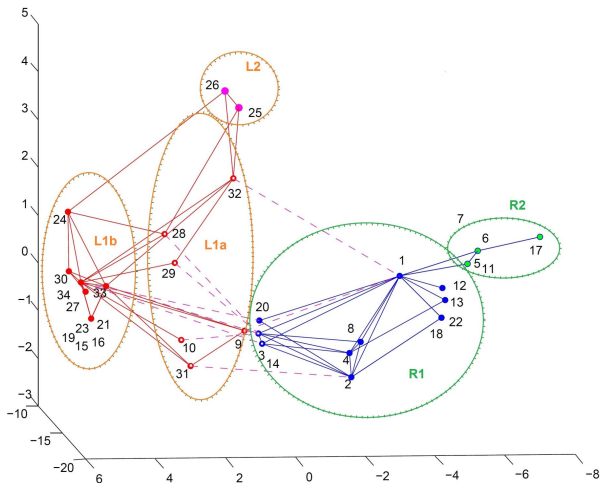


Fig. 15. Hierarchical structure of Karate club network is marked with different ellipses. Two first level communities are L and R. Four second level communities are L1, L2, R1, R2 and four third level communities are L1a, L1b, R1a, R1b.

We observe $L1a$ to be a disconnected community however the nodes $\{9, 10, 28, 29, 31, 32\}$ are globally close. There are no direct links between three groups $\{28, 29, 32\}$, $\{9, 31\}$ and $\{10\}$. The global similarity can be visually observed from Figure 15 where all nodes in $L1a$ are closer to the R while the nodes in $L1b$ are relatively distant from R . A further increase $K = 6$ caused a split of $R1$ to $R1a$ and $R1b$. The three nodes of $R1$ $\{3, 14, 20\}$ are close to the boundary of L and R communities. The nodes $\{3, 14\}$ split from rest of the nodes and formed a new community $R1b$ which makes the third level of hierarchy.

These experiments demonstrate the capability of the proposed GDG algorithm to detect hierarchical communities. Note that the hierarchical structure is not imposed rather only the number of communities are varied and communities are independently found each time.

4.5 Consistency of Community Occupancy

We also performed consistency of community-occupancy analysis by varying the number of communities and computing the occupancy map each time. The occupancy map M_o has size $n \times n$ and $M_o(i, j) = 1$ if a pair of nodes i, j is in the same community, otherwise $M_o(i, j) = 0$. Integration of all occupancy maps yielded an overall map showing the pairs which were for a given number of times in the same community. For the Karate Club network we varied the number of communities as $K = \{2, 3, 4, 5, 6\}$. The integrated occupancy map and histogram of node pairs based on consistency is shown in Figure 16. In this network we observe 19.55% of the pairs remained 100% consistent while 52.768% pairs never existed. Due to hierarchical community structure, as the communities are increased from 2 to 6, the occupancy pattern changes significantly. Based on consistency, we can classify the node pairs being never in the same community, or a given number of times in the same community. Such a classification of nodes pairs is shown in Figure 16a, in which each class is shown by a different color. The color to consistency mapping is shown in the histogram where color of a bar encodes the consistency value and length of the bar represents the probability of the node pairs of a particular consistency. By using this analysis we identify the core

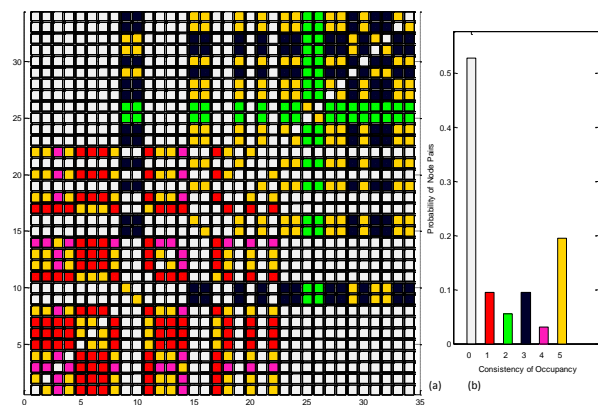


Fig. 16. (a) Integrated consistency map of Karate Club network for $K = \{2, 3, 4, 5, 6\}$ and $b_w = 1.0$. (b) Consistency histogram.

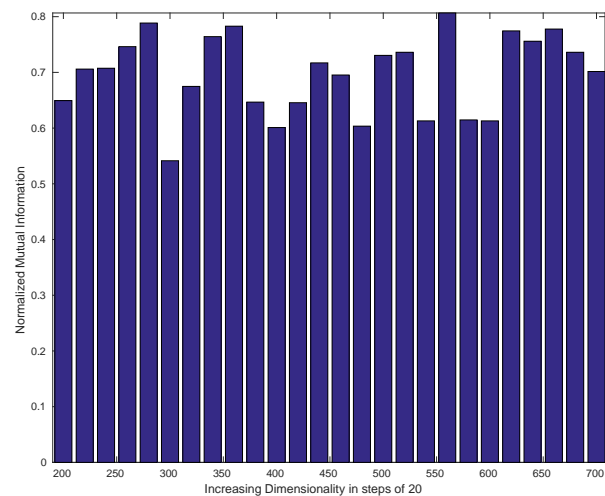


Fig. 17. NMI between the original communities and the low dimensional communities in the Asia MidEast network, starting from 200 dimensional subspace.

of each community which are most consistent set of nodes in that community.

4.6 Scalability of the Proposed Algorithm to Bigger Networks

As the number of nodes in a network increases, the dimensionality of the corresponding geodesic space will also increase. In very high dimensional spaces, the performance of clustering algorithms may degrade. To make the proposed algorithm applicable to bigger networks, dimensionality reduction needs to be performed over the geodesic space. In this section, we consider PCA for dimensionality reduction. We find the principal components of the geodesic space and project all geodesic vectors on $p < n$ principal dimensions. As a result, we get p dimensional geodesic space. We apply the proposed algorithm in this space. Comparison of the communities found in low-dimensional space with the original communities reveals a good match in most cases, as discussed below.

We have applied PCA based dimensionality reduction technique to various networks and studied the performance of the

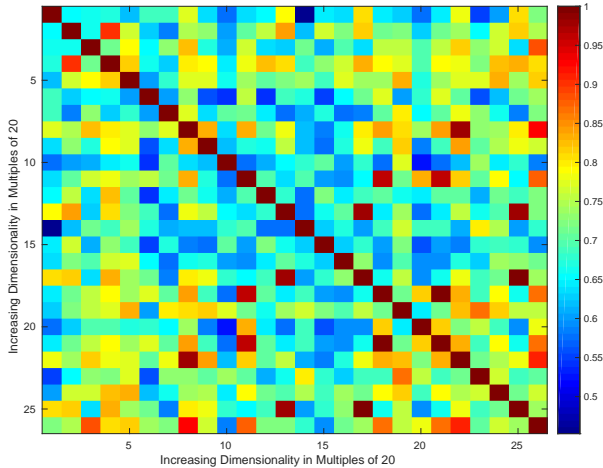


Fig. 18. NMI across low dimensional communities in the Asia MidEast network shown as heat-map. Starting dimensionality shown as 1 is 200 dimensional space. Each increment is of 20 dimensions in the order of reducing eigenvalues.

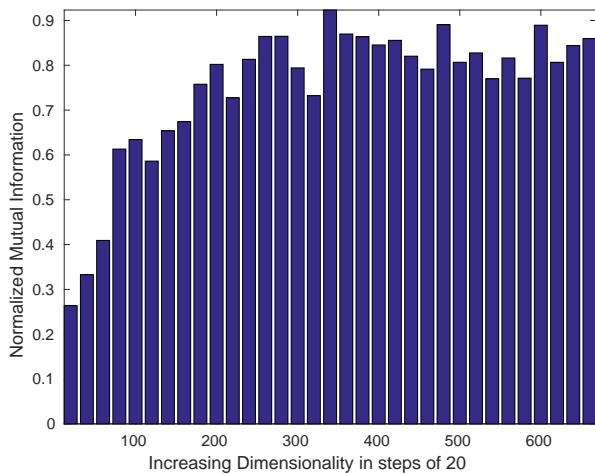


Fig. 19. NMI between the original communities and the low dimensional communities in the Yeast network, starting from a 20 dimensional subspace. NMI increases with the increasing dimensionality from 20 to 300 dimensions. Beyond that NMI remains almost the same.

proposed algorithm by varying the dimensionality of the space. We used Normalized Mutual Information (NMI) to find the similarity between the communities found in reduced dimensionality spaces and the original communities. The Asia MidEast network has 706 nodes. See details of the network in Table 1. By using the proposed DGD algorithm, 13 communities were found corresponding to the minimum clustering error gradient. We projected the network to $\{200, 220, \dots, 700\}$ dimensional spaces and independently identified 13 communities in each subspace. Then NMI is computed between the communities in each subspace and the original communities, as shown in Figure 17. In this experiment, the average NMI is 0.70 ± 0.072 . Communities found for the low-dimensional sub-spaces are also compared with each other and the resulting NMI has been shown as a heat map in Figure 18. The overall average NMI is 0.721 ± 0.1043 .

Similar experiments have also been performed for the Yeast network having 662 nodes. See details of the Yeast network in Table 1. We varied the dimensionality of the geodesic space

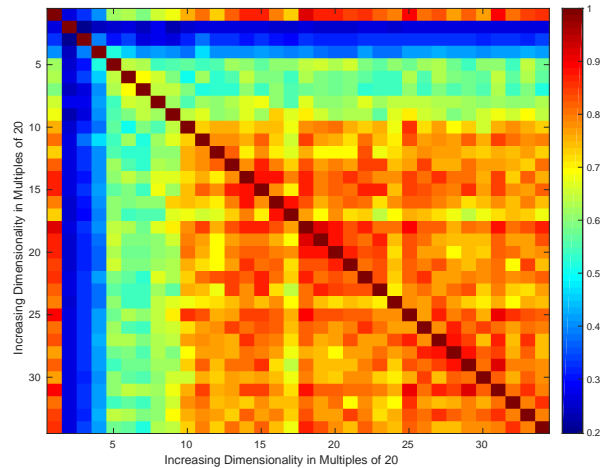


Fig. 20. NMI across low dimensional communities in the Yeast network shown as heat-map. The second row and 2nd column are the starting dimensionality which is 20 dimensional space. Each increment is of 20 dimensions in the order of reducing eigenvalues. First column and first row show the NMI between each lower dimensional community with the full dimensionality communities.

as follows $\{20, 40, \dots, 660\}$. For each dimensionality, network is divided into 21 communities. NMI computed between the communities found in low-dimensional subspace and the original communities is shown in Figure 19. The average NMI is found to be 0.7508 ± 0.158 . We observe a higher NMI for subspaces with dimensionality 200 or more. In this case, average NMI is 0.7915 ± 0.0452 . NMI found between low dimensional communities is shown as a 2D heat map in Figure 20. In this experiment, overall average NMI is 0.6731 ± 0.1843 . NMI between communities in 200 dimensional sub-spaces or higher has average 0.7813 ± 0.100 . The first column and first row in this map is the NMI of each low dimensional set of communities with the original communities.

These experiments demonstrate that a dimensionality reduction technique preserving distances between the points as in the original space will result in higher similarity between the communities in the low dimensional space and the communities in the original space.

4.7 Execution Time Comparisons

Execution time of the proposed GDG algorithm has been compared with two recent algorithms GSSC and SSCF [35] for six different networks on Intel 2.7GHz quad-core i5 processor machine with 16GB RAM as shown in Figure 21. For smaller networks such as Karate and Football the three algorithms are quite fast. For the synthetic LFR network having 1000 nodes, the execution time of both GSSC and SSCF increases with the increasing value of the mixing parameter μ . However the proposed GDG algorithm is not much effected due to increased network complexity. For the case of polblog network having 1490 nodes the proposed GDG algorithm has performed much faster than the subspace based algorithms. It is because the performance of subspace based algorithms is dependent on the the network complexity while the proposed algorithm is not much effected.

5 CONCLUSION

Many real world complex systems can be easily mapped to networks instead of geometric spaces because only the presence or

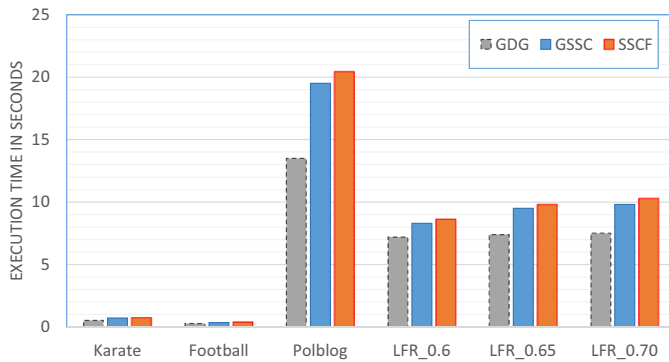


Fig. 21. Execution time of the proposed GDG algorithm compared with two recent algorithms GSSC and SSCF [35] on three real networks (Karate (nodes=34, edges=78), Football(nodes=115, edges=631), Polblog(nodes=1490, edges=16716)) and three synthetic networks (LFR $\mu = \{0.60, 0.65, 0.70\}$ (nodes=1000, edges=9774)). The proposed GDG algorithm is faster than both of these current algorithms.

absence of a link between two entities is known. For recognition of structural patterns in these systems, the network nodes need to be mapped to a geometric space. In this paper we proposed using geodesic distance vectors for this purpose. A *Geodesic Density Gradient (GDG)* algorithm is proposed to find communities and to reduce the error at the community boundaries.

The proposed GDG algorithm is based on a distance measure specifically designed for improved community detection in geodesic space. Each node in the geodesic space is shifted towards a positive density gradient until convergence is obtained overall nodes. In a post processing step, the number of communities is increased from a minimum value ($k \geq 2$) to a larger number and the variation of the clustering error derivative is observed. Initially the error derivative decreases rapidly and then it slows down and after a particular number of communities the error derivative becomes less than a threshold yielding the number of communities.

The variation of the number of communities gave an opportunity to study hierarchical community structure. As the number of communities is increased, coarser communities split into finer ones revealing a hierarchical community structure in the network. Splitting of coarser communities is not forced rather the optimization is independently applied for increased number of communities. A perfect hierarchical structure was observed in some real world networks such as Karate club network and the Dolphin social network.

Consistency of community occupancy is also studied by varying the number of communities and counting the co-occupancy of each pair of nodes. Node pairs having very high consistency form the core of each community. The nodes which are outside the core may switch partitions and therefore may be considered members of more than one community as is the case of overlapped community structure.

The focus of the current work has remained on non-overlapped community detection by considering a node to be member of only one community at a time. An important future goal of our research is to extend it for overlapped and time varying community detection.

ACKNOWLEDGMENTS

This work is funded by an Australian Research Council Discovery Project (DP140100203). M. Small is supported by an Australian

Research Council Future Fellowship (FT110100896).

REFERENCES

- [1] L. Adamic and N. Glance. The political blogosphere and the 2004 US election: divided they blog. *Proc. 3rd Int. Workshop on Link Discovery*, 411:36–43, 2005.
- [2] M. Ankerst, M. M. Breunig, H.-P. Kriegel, and J. Sander. Optics: ordering points to identify the clustering structure. In *ACM Sigmod Record*, volume 28, pages 49–60. ACM, 1999.
- [3] A. L. Barabasi. *Network Science* (online available: barabasilab.neu.edu/networksciencebook). 2012.
- [4] V. D. Blondel, J.-L. Guillaume, R. Lambiotte, and E. Lefebvre. Fast unfolding of communities in large networks. *J. Stat. Mech.: Theory Exp.*, page P10008, 2008.
- [5] R. F. Cancho, C. Janssen, and R. V. Sole. Topology of technology graphs: Small world patterns in electronic circuits. *Phys. Rev. E*, 64:046119, 2001.
- [6] J. Chen and Y. Saad. Dense subgraph extraction with application to community detection. *IEEE TKDE*, 24(7):1216–1230, July 2012.
- [7] Y. Cheng. Mean shift, mode seeking, and clustering. *Pattern Analysis and Machine Intelligence, IEEE Transactions on*, 17(8):790–799, 1995.
- [8] A. Clauset, M. E. J. Newman, and C. Moore. Finding community structure in very large networks. *Phys. Rev. E*, 70:066111, 2004.
- [9] D. Comaniciu and P. Meer. Mean shift: A robust approach toward feature space analysis. *Pattern Analysis and Machine Intelligence, IEEE Transactions on*, 24(5):603–619, 2002.
- [10] L. Danon, A. Daz-Guilera, and A. Arenas. The effect of size heterogeneity on community identification in complex networks. *J. Stat.*, 2006.
- [11] D. Deritei, Z. I. Lázár, I. Papp, F. Járαι-Szabó, R. Sumi, L. Varga, E. R. Regan, and M. Ercsey-Ravasz. Community detection by graph voronoi diagrams. *New Journal of Physics*, 16(6):063007, 2014.
- [12] L. Donetti and M. A. Munoz. Detecting network communities: a new systematic and efficient algorithm. *Journal of Statistical Mechanics: Theory and Experiment*, 2004(10):P10012, 2004.
- [13] M. Ester, H.-P. Kriegel, J. Sander, and X. Xu. A density-based algorithm for discovering clusters in large spatial databases with noise. In *Kdd*, volume 96, pages 226–231, 1996.
- [14] S. Fortunato. Community detection in graphs. *Physics Reports*, 486(3):75–174, 2010.
- [15] S. Fortunato and M. Barthlemy. Resolution limit in community detection. *Proc. Natl. Acad. Sci. USA*, 104:36–41, 2007.
- [16] M. V. Fragkiskos D. Malliaros. Clustering and community detection in directed networks: A survey. *Physics Reports*, 533(4):95–142, 2013.
- [17] M. Girvan and M. E. Newman. Community structure in social and biological networks. *Proceedings of the National Academy of Sciences*, 99(12):7821–7826, 2002.
- [18] M. Girvan and M. E. J. Newman. Community structure in social and biological networks. *Proceedings of the National Academy of Sciences*, 99(12):7821–7826, 2002.
- [19] P. M. Gleiser and L. Danon. Community structure in jazz. *Advances in complex systems*, 6(04):565–573, 2003.
- [20] M. Gong, J. Liu, L. Ma, Q. Cai, and L. Jiao. Novel heuristic density-based method for community detection in networks. *Physica A: Statistical Mechanics and its Applications*, 403:71–84, 2014.
- [21] R. Guimer, M. Sales-Pardo, and L. A. N. Amaral. Classes of complex networks defined by role-to-role connectivity profiles. *Nature Physics*, 3:63–61, 2007.
- [22] R. Guimer, S. Mossa, A. Turtschi, and L. A. N. Amaral. The worldwide air transportation network: Anomalous centrality, community structure, and cities’ global roles. *Proceedings of the National Academy of Sciences*, 102(22):7794–7799, 2005.
- [23] J. H. M. S. B. A. L. and O. Z. N. Lethality and centrality in protein networks. *Nature*, 411, 2001.
- [24] N. Halko, P.-G. Martinsson, Y. Shkolnisky, and M. Tytgert. An algorithm for the principal component analysis of large data sets. *SIAM J. Sci. Comput.*, 33(5):2580–2594, Oct 2011.
- [25] X. Jiang, H. Wang, S. Tang, L. Ma, Z. Zhang, and Z. Zheng. A new approach to shortest paths on networks based on the quantum bosonic mechanism. *New Journal of Physics*, 13:013022, 2013.
- [26] H. Jin, S. Wang, and C. Li. Community detection in complex networks by density-based clustering. *Physica A: Statistical Mechanics and its Applications*, 392(19):4606–4618, 2013.
- [27] J. N. Kaftan, A. A. Bell, and T. Aach. Mean Shift Segmentation Evaluation of Optimization Techniques. In *Proceedings of the Third International Conference on Computer Vision Theory and Applications, VISAPP 2008*, pages 365–374, Funchal, Madeira - Portugal, January 22–25 2008. INSTICC - Institute for Systems and Technologies of Information, Control and Communication.

- [28] A. Lancichinetti and S. Fortunato. Community detection algorithms: a comparative analysis. *Physical review E*, 80(5):056117, 2009.
- [29] A. Lancichinetti and S. Fortunato. Limits of modularity maximization in community detection. *Physical Review E*, 84(6):066122, 2011.
- [30] A. Lancichinetti, S. Fortunato, and J. Kertész. Detecting the overlapping and hierarchical community structure in complex networks. *New Journal of Physics*, 11(3):033015, 2009.
- [31] A. Lancichinetti, S. Fortunato, and F. Radicchi. Benchmark graphs for testing community detection algorithms. *Phys. Rev. E*, 78(4):046110, 2008.
- [32] J. Leskovec, J. Kleinberg, and C. Faloutsos. Graph evolution: Densefication and shrinking diameters. *ACM Transactions on Knowledge Discovery from Data (ACM TKDD)*, 1(1), 2007.
- [33] D. Lusseau. The emergent properties of a dolphin social network proc. *Proc. R. Soc. London, Ser. B (Suppl.)*, 270:S186, 2003.
- [34] D. Lusseau, K. Schneider, O. J. Boisseau, P. Haase, E. Slooten, and S. M. Dawson. *Behav. Ecol. Sociobiol.*, 54:396, 2003.
- [35] A. Mahmood and M. Small. Subspace based network community detection using sparse linear coding. *TKDE*, 28(3):801–812, March 2016.
- [36] R. Milo, S. Shen-Orr, S. Itzkovitz, N. Kashtan, D. Chklovskii, and U. Alon. Network motifs: Simple building blocks of complex networks. *Science*, 298(5594):824–827, 2002.
- [37] M. Newman. *Networks: an introduction*. Oxford University Press, 2010.
- [38] M. E. Newman and M. Girvan. Finding and evaluating community structure in networks. *Physical review E*, 69(2):026113, 2004.
- [39] M. E. J. Newman. Finding community structure in networks using the eigenvectors of matrices. *Phys Rev. E*, 74(3):036104, 2006.
- [40] M. E. J. Newman and E. A. Leicht. Mixture models and exploratory analysis in networks proc. *Natl. Acad. Sci. USA*, 104:9564–9569, 2007.
- [41] T. Nishikawa and A. E. Motter. Discovering network structure beyond communities. *Scientific reports*, 1, 2011.
- [42] G. Palla, I. Dernyi, I. Farkas, and T. Vicsek. Uncovering the overlapping community structure of complex networks in nature and society. *Nature (London)*, 435:814–818, 2005.
- [43] S. Pettie and V. Ramachandran. A shortest path algorithm for real-weighted undirected graphs. *SIAM Journal on Computing*, 34(6):1398–1431, 2005.
- [44] F. Radicchi. A paradox in community detection. *EPL*, 106:38001, 2014.
- [45] F. Radicchi, C. Castellano, F. Cecconi, V. Loreto, and D. Parisi. Defining and identifying communities in networks proc. *Natl. Acad. Sci. USA*, 101:2658–2663, 2004.
- [46] P. Ronhovde and Z. Nussinov. Multiresolution community detection for megascale networks by information based replica correlations. *Phys. Rev. E*, 80:016109, 2009.
- [47] M. Rosvall and C. T. Bergstrom. An information-theoretic framework for resolving community structure in complex networks proc. *Natl. Acad. Sci. USA*, 104:7327–7331, 2007.
- [48] S. van Dongen. *Graph clustering by flow simulation*. Ph.D. Thesis, Dutch National Research Institute for Mathematics and Computer Science, University of Utrecht, Netherlands, 2000.
- [49] D. Watts and S. Strogatz. Collective dynamics of ‘small-world’ networks nature. *Nature*, 393:440–442, 1998.
- [50] W. Zachary. An information flow model for conflict and fission in small groups. *Journal of anthropological research*, 33(4):452–473, 1977.



Arif Mahmood Arif received his Masters and the Ph.D. degrees in Computer Science from the Lahore University of Management Sciences in 2003 and 2011 respectively with distinction. Currently he is Postdoc researcher in the Department of Computer Science and Engineering, Qatar University. The research work presented in this manuscript was mainly performed while he was Research Assistant Professor with the School of Mathematics and Statistics, the University of the Western Australia (UWA). He is

keenly interested in exploring the applications of Machine Learning techniques for the complex network structure characterization. Before that he was Research Assistant Professor with the College of Computer Science and Software Engineering, UWA. His major research interests are in Computer Vision and Pattern Recognition. More specifically he has performed research in data clustering, classification, action and object recognition using image sets, scene background modeling, and person segmentation and action recognition in crowds. He has also worked on the computation elimination algorithms for fast template matching, image segmentation and facial expression mapping.



Michael Small Michael is the CSIRO-UWA Chair at Complex Engineering Systems. Previous to this he was awarded an Australian Research Council (ARC) Future Fellowship and he was Winthrop Professor in Applied Mathematics in the School of Mathematics and Statistics at the University of Western Australia (UWA). His academic career began with undergraduate and doctoral degrees in Pure and Applied Mathematics at UWA, after a string of post-doc appointments he joined the faculty of the Department of

Electronic and Information Engineering of the Hong Kong Polytechnic University (2001-2011). In 2012 he moved back to UWA. He is a Senior Member of IEEE and on the editorial board of several international journals including Chaos, Int. J. of Bifurcation and Chaos, IEEE Transactions on Circuits and Systems II. His research interests are in: complex systems, complex network, chaos and nonlinear dynamics, nonlinear time series analysis and computational modelling. Applications of his research include: phenomics, genomics, physiology, biomedical signal processing, financial analysis, granular mechanics, animal movement and behaviour, epidemiology and mechanical systems.

Somaya Ali Al-Maadeed Somaya is the head of Computer Science (CS) Department at Qatar University. She is IEEE Qatar Section Chair and the coordinator of Computer Vision research group at Qatar University. She received her PhD in CS from Nottingham University UK in 2004. She has received letter of thanks from Sheikh Tamim bin Hamad Al Thani for her work in Biometric Security. Her team is the recipient of the best performance in ICDAR2011 and ICDAR2015 signature verification contest. She is a visiting academic at Northumbria University, UK. She has organized several workshops and competitions related to biometrics and computer vision. She has served as Technical Chair of several international conferences. She is an associate editor at IET Image Processing Journal and guest editor of Journal of Electrical and computer Engineering. She has been selected as a participant in Current and Future Executive Leaders Program at Qatar Leadership Centre. She is PI of several funded research projects generating approximately five million dollars in the last three years. She has delivered a number of workshops on teaching and research. She is a senior IEEE member and a member of other Engineering Societies including IEEE Women in Engineering, IEEE Education Society, and IEEE Electric Vehicles.



Nasir Rajpoot Nasir is Professor in the Department of Computer Science at the University of Warwick. He also holds the Honorary Pathology Scientist position at the University Hospitals Coventry & Warwickshire NHS Trust. He received his PhD in digital image processing from the University of Warwick in 2001. During 1998-2000, he was a postgraduate research fellow in the Applied Mathematics program at Yale University, USA. He is the founding Head of Tissue Image Analytics lab (formerly BIA lab) at War-

wick. Current focus of research in his lab is on developing algorithms for the analysis of gigapixel digital pathology images, with applications to computer-assisted grading of cancer and image-based markers for prediction of cancer progression and survival. His group won the MITOS-ATYPIA challenge contest on nuclear atypia scoring in breast cancer histology images held in conjunction with ICPR'2014, and was ranked among the top three contestants in the AMIDA challenge contest on mitotic cell detection in breast histology images held in conjunction with MICCAI'2013. Recently, a paper by his lab on the detection of epithelial tumour cells in cancer histology images won the Best Paper award at the Patch-based Medical Imaging (PMI) workshop held in conjunction with MICCAI'2015. Prof Rajpoot has co-chaired several meetings in the area of histopathology image analysis (HIMA) since 2008. He was the General Chair of the UK Medical Image Understanding and Analysis (MIUA) conference in 2010, and the Technical Chair of the British Machine Vision Conference (BMVC) in 2007. He has guest edited a special issue of Machine Vision and Applications on Microscopy Image Analysis and its Applications in Biology in 2012, and a special section on Multivariate Microscopy Image Analysis in the IEEE Transactions on Medical Imaging in 2010. He is a Senior Member of IEEE and member of the ACM, the British Association of Cancer Research (BACR), and the European Association of Cancer Research (EACR).